Electrochimica Acta 383 (2021) 138356

Contents lists available at ScienceDirect

Electrochimica Acta

journal homepage: www.elsevier.com/locate/electacta

Understanding the capacitance of thin composite films based on conducting polymer and carbon nanostructures in aqueous electrolytes

Anita Cymann-Sachajdak[a], Magdalena Graczyk-Zajac[b,#], Grzegorz Trykowski[c], Monika Wilamowska-Zawłocka[a,*]

[a] Department of Energy Conversion and Storage, Faculty of Chemistry, Gdańsk University of Technology, Narutowicza 11/12, Gdańsk 80-233, Poland
[b] Fachbereich Material und Geowissenschaften, Technische Universität Darmstadt, Otto-Berndt-Straße 3, Darmstadt 64287, Germany
[c] Faculty of Chemistry, Nicolaus Copernicus University in Toruń, Gagarina 7, Toruń 87-100, Poland

ARTICLE INFO

Article history:
Received 10 January 2021
Revised 29 March 2021
Accepted 3 April 2021
Available online 9 April 2021

Keywords:
Composite electrode materials
Conducting polymer
Graphene oxide
Carbon nanotubes
Electrolytes
Electrochemical capacitors

ABSTRACT

In this work electrochemical performance of thin composite films consisted of poly(3,4-ethylenedioxythiophene) (PEDOT), graphene oxide (GOx) and oxidized multiwalled carbon nanotubes (oxMWCNTs) is investigated in various sulphates (Li_2SO_4, Na_2SO_4, K_2SO_4, $MgSO_4$) and acidic (H_2SO_4) electrolytes. Capacitance values, rate capability and cycling stability achieved for the composite layers are correlated with the electrolytes' properties such as the conductivity, viscosity, cation size and pH. The highest capacitance values are achieved in acidic solution (98.6 mF cm^{-2} at 1 mA cm^{-2}), whereas cycling stability is better in neutral electrolytes (88.4% of initial capacitance value after 10′000 cycles recorded for symmetric supercapacitor in 0.5 M $MgSO_4$ solution). Diffusion controlled and non-diffusion controlled capacitance contributions are calculated and the results are discussed considering various ranges of sweep rates taken into account in the linear fitting and extrapolation of parameters.

1. Introduction

A great demand for high power and high energy storage devices drives development of new electrode materials of improved electrochemical properties as well as stable electrolytes. There are two ways to increase the energy of the device by enhancing the capacitance or widening the working voltage. Hence, it is very important to match the electrolyte to the properties of the electrode material in order to achieve the highest capacitance along with the stable work of the device [1–4]. Therefore, it is crucial to understand the charge storage mechanisms in various electrolytes. Electrolytes are divided into three main types: aqueous, organic and ionic liquid. The aqueous ones are advantageous compared to the other two types in terms of conductivity, viscosity and environmental issue. The major drawback, however, is a low potential range of their stability limited by the thermodynamic decomposition voltage of water (1.23 V). Still, neutral aqueous electrolytes are stable in wider potential range than acidic or basic ones. Moreover, using concentrated electrolytes one can increase the useful potential range above the voltage of theoretical decomposition of water. For instance, 1.9 V was achieved for 0.3 M K_2SO_4 when unequal mass of negative and positive electrodes was implemented [5], 2.2 V for 1 M Li_2SO_4 using gold current collectors [6], and 3.2 V for saturated $NaClO_4$ on glassy carbon substrate [4]. Naderi et al. achieved 2.8 V for flexible asymmetric capacitor based on conducting polymer/reduced graphene oxide/MnO_2 nanocomposites with water-in-salt electrolyte (27 mol kg^{-1} potassium acetate) [7]. The combination of higher capacitances obtained in aqueous electrolytes than in organic ones or ionic liquids along with the wide operating potential range leads to a high energy density of the device.

The electrolyte choice has a great impact on capacitance, energy and power values as well as cyclability of energy storage devices. Ion size and its mobility is crucial for electric double layer capacitors (EDLCs), where physical adsorption of ions on the electrode surface determines the capacitance values. For this reason, new electrode materials with tunable porosity are developed to match the pore sizes with the ionic radii of the electrolyte ions [8–11]. In the case of electrodes operating only with non-faradaic processes, the electrolyte properties are key factors to utilize the whole specific surface area. Also, electrochemical performance of pseudocapacitive materials, such as conducting polymers or transi-

* Corresponding author.
E-mail address: monika.wilamowska@pg.edu.pl (M. Wilamowska-Zawłocka).
Present address: EnBW Energie Baden-Württemberg AG, Durlacher Allee 93, 76131 Karlsruhe, Germany

https://doi.org/10.1016/j.electacta.2021.138356

tion metal oxides, that involve faradaic reactions is influenced by ion size, pH, conductivity and viscosity of electrolytes.

Electroactive polymers are attractive components of composite electrode materials due to their excellent properties such as high conductivity in doped state, pseudocapacitive behaviour, fast kinetics of oxidation and reduction processes and flexibility [12–14]. They play a role of conducting binder and a matrix for other electroactive components. Electroactive polymers are conducting only in their doped state with counter-ions balancing the charge of the polymer chains. In p-type electroactive polymers, such as poly(3,4-ethylenedioxythiophene (PEDOT), polyaniline (PANI) or polypyrrole (PPy), anions compensate the charge of polarons and bipolarons created during oxidative polymerisation, so they behave as anion exchangers [15,16]. Bund and Neudeck observed migration of anions and solvent molecules upon doping/dedoping processes of poly(3,4-ethylenedioxythiophene) films in various electrolytes, with no significant exchange of cations [15]. When large polyanions (e.g. polystyrene sulfonate (PSS)) or macromolecule counterions (e.g. graphene oxide) are introduced during polymerization process, p-type polymers act as cation exchangers [16–18]. However, migration of cations are noticed also in polymer layers without large anions trapped inside them, as observed by Gruia et al. in the case of PEDOT films with ClO_4^- counter ions [19] or by Jureviciute et al. for poly(vinylferrocene) films in aqueous perchlorate solutions [20]. Therefore, it is crucial to investigate electrochemical performance of electroactive polymers and polymer-based composites in various electrolytes as migration of ions and solvent molecules influence properties of the polymer films such as electrochemical response, ionic conductivity, morphology, stiffness, etc. [19,21–23].

Composites based on PEDOT and carbonaceous materials have attracted attention as electrodes for supercapacitors due to good electrochemical and thermal stability, high capacitance values, and good rate capability [24–32]. As we showed in our recent work [29], ternary composites that combine two different carbonaceous materials and conducting polymer exhibit improved electrochemical properties compared to the analogous binary composites. Electrochemical performance of such ternary composites depends strongly on their microstructure, morphology, ratio between the components, adhesion to the electrode substrate etc. [26,29,33]. In majority of works related to composites based on conducting polymer and carbonaceous materials, the main focus is on the micro-nanostructure, chemistry and ratio of components and their influence on the electrochemical properties of the final composites, while the presented electrochemical performance is often limited to one or two electrolyte solutions.

In this work we present thorough electrochemical study of ternary PEDOT/GOx/oxMWCNTs composites in various aqueous electrolytes containing different cations: Li^+, Na^+, K^+, Mg^{2+}, H^+ and the same anion SO_4^{2-}. Capacitance values, rate capability and cycling stability are discussed taking into account electrolytes' properties such as pH, conductivity, viscosity and effective ion size. We evaluate the electrochemical results to differentiate diffusion controlled and non-diffusion controlled contributions to capacitance values using Trasatti's analysis [34,35] as well as equation proposed by Conway [36]. Moreover, we discuss the achieved values depending on sweep rate range taken into account in the linear fitting and extrapolation of parameters in both methods, which is not debated in literature.

2. Experimental

2.1. Chemicals

Monomer 3,4-ethylenedioxythiophene (EDOT) and multiwalled carbon nanotubes —MWCNTs (≥98% carbon basis, O.D. × *I.D.* × *L* 10 nm ± 1 nm × 4.5 nm ± 0.5 nm × 3-~6 μm) were purchased from Sigma–Aldrich (Merck KGaA, Darmstadt, Germany) and used as received. The suspension of graphene oxide (4.5 mg/mL) was prepared via modified Hummers method (supplied by Institute of Electronic Materials Technology (ITME), Warsaw, Poland). Inorganics: Li_2SO_4, Na_2SO_4, K_2SO_4, and concentrated acids: H_2SO_4 (98 wt.%), HNO_3 (65 wt.%) (Avantor Performance Materials Poland S.A., Gliwice, Poland) were of analytical grade and used without any further purification. Water-based electrolytes were prepared using deionized water.

2.2. Preparation of the thin composite films

The composite PEDOT/GOx/oxMWCNTs films were electrodeposited from an aqueous suspension of carbonaceous materials containing EDOT monomer, as described in our recent work [29]. Briefly, pure MWCNTs were chemically oxidized with concentrated HNO_3 (24 h, 130 °C), washed, filtrated and dried (overnight, 80 °C) under vacuum conditions. Afterwards, 5 mg of modified carbon nanotubes and 80 μL of EDOT monomer (0.015 mol dm^{-3}) were added to the 30 ml of deionized water (conductivity < 0.06 μS) and sonicated for 3 min (amplitude 50%, power 25 W) with Ultrasonic Lab Homogenizer (UP200St, LT Scientific, Hielscher). In the next step 11.11 ml of graphene oxide suspension (4.5 mg/ml) and appropriate amount of deionized water was added to the mixture of CNTs and monomer to obtain 50 ml of the synthesis solution. Before the electrodeposition process, the solution was stirred with magnetic stirrer and deaerated with argon for 1 h. The solution was also stirred (800 rpm) during the deposition process to ensure homogeneity of the composites layers. The films were electrodeposited in the three-electrode system at a constant potential of 1 V vs. Ag|AgCl|0.1 M KCl on the working electrode (glassy carbon (GC), 2 mm in diameter) or platinum plates (area of 1 cm^{-2}). Pt mesh and Ag|AgCl|0.1 M KCl served as a counter and reference electrode, respectively. The deposition process was controlled by the deposition charge (cut-off at 0.8 C cm^{-2}). Afterwards, the prepared composite films were washed carefully with deionized water, immersed into the water-based electrolyte solution and reduced electrochemically at −0.6 V vs. ref Ag|AgCl|3 M KCl for 5 min. Electrochemical reduction process causes partial reduction of graphene oxide component, as described in our former works [28,29].

2.3. Characterisation techniques

The structure and morphology of the electrodeposited PEDOT/GOx/oxMWCNTs layers were investigated using scanning electron microscope (accelerating voltage equal to 20 kV) with a secondary electrons detector (FEI Quanta FEG 250 Scanning Electron Microscope (SEM), ThermoFischer Scientific, Waltham, MA, USA) and transmittance electron microscope (TEM, FEI Europe, TecnaiF20 X-Twin). The total porosity and the pore size distribution of the composite samples were determined by the Brunauer-Emmett-Teller (BET) method using NOVAtouchNT-LX-1 Qunatachrome Instruments analyser (Anton Paar GmbH). Conductivity of the electrolytes were measured on CPC-500 conductometer (ELMETRON, Zabrze, Poland).

Electrochemical measurements were carried out in two- and three-electrode cell configuration using SP-200 potentiostat/galvanostat (Bio-Logic, Seyssinet-Pariset, France) under EC-Lab Software (V11.31 version). In three-electrode setup Pt mesh and Ag|AgCl|3.0 M KCl served as counter and reference electrodes, respectively. For two-electrode measurements a symmetric device was assembled in SWAGELOK®-type cell. Two composite layers deposited on glassy carbon were separated with filter paper (Macherey Nagel, 300 μm in thickness, MN GF – 1) soaked with the electrolyte. Calculation of capacitance values based on cyclic

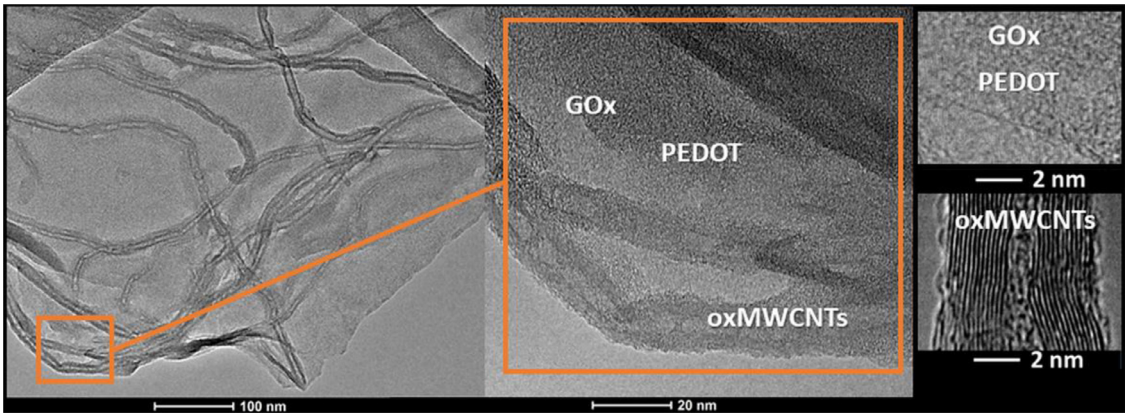

Fig. 1. TEM images of PEDOT/GOx/oxMWCNTs composite.

voltammetry, chronopotentiometry and electrochemical impedance spectroscopy are given in Eq. S1-S3 in Supplementary Materials (SM).

3. Results and discussion

Physicochemical characterisation of PEDOT/GOx/oxMWCNTs composites and influence of amount of oxMWCNTs on the composites' properties were described in our former work [29]. Fig. 1 presents TEM images of the composite PEDOT/GOx/oxMWCNTs. The picture shows multiwalled carbon nanotubes with a diameter of 13 nm and visible 13 walls dispersed in PEDOT/GOx thin film.

Specific surface area of PEDOT/GOx/oxMWCNTs composite calculated from BET analysis is equal to 8.3 $m^2\ g^{-1}$, and the total pore volume equals to 0.006 $cm^3\ g^{-1}$. Such a small value is often reported for PEDOT and PEDOT-based composites [37,38,39]. The BET adsorption/desorption hysteresis loop is presented in Fig. S1 (SM). The pore size distribution (Inset in Fig. S1, SM) show that the material is meso– and macroporous with the highest number of pores 8 nm in size.

Electrochemical properties of the PEDOT/GOx/oxMWCNTs films were investigated in different sulphates (Li_2SO_4, Na_2SO_4, K_2SO_4, $MgSO_4$) and acidic (H_2SO_4) aqueous electrolytes (concertation of 0.5 mol dm^{-3}). Properties such as pH, conductivity and viscosity of the used electrolytes are given in Table S1 (in SM). Acidic solution exhibits the highest conductivity (197.1 mS cm^{-1}), whereas amongst the neutral ones K_2SO_4 shows the highest value (74.7 mS cm^{-1}). The reason of the much higher conductivity value for H_2SO_4 is a different mechanism of proton transport [40,41] compared to neutral ions. In the case of Li, Na and K sulphates the number of ions in electrolytes of equal concentration is the same, so their mobility determines the ionic conductivity - as the size of the hydrated ion increases, its mobility, and thus its conductivity, decreases. Aqueous solution of magnesium sulphate has ability to form strong ion pairs, thus it as a model compound to investigate ion association [42,43]. Moreover, higher cation charge of magnesium ion, compared to Li, K and Na, is more influenced by the external electric field, which increases ion mobility. On the other hand, greater interaction of Mg^{2+} ion with water and larger hydration sphere decrease its mobility, hence its low conductivity (31.2 mS cm^{-1}). Ion size is also important for the efficient charge storage by electric double layer formation as well as for diffusion of ions in the electrode material. The size of ion in aqueous solution can be determined by different methods, thus the values reported in the literature differ for the same ion [9,44–49]. The ionic radii in solids (R_{ion}) and effective ionic radii in solution ($d_{i\text{-}w}$ - determined as an internuclear distance between metal ion and oxygen from water molecule) of the investigated electrolytes' ions are presented in Table S2 and Table S3 (in SM). Despite the differences in absolute values, the increase in the effective ionic radii follows the trend: $Li^+ < Mg^{2+} < Na^+ < K^+$.

Electrochemical performance of PEDOT/GOx/oxMWCNTs film measured in three-electrode cell configuration is presented in Fig. 2. The shape of cyclic voltammetry curves slightly differ in various electrolytes (Fig. 2a). The deviation of the CV curve from the rectangular shape is increasing in the following direction: K_2SO_4 < Na_2SO_4 < Li_2SO_4 < $MgSO_4$. This illustrates the cation transport in the composite layer. The highest deviation from the rectangular shape, which corresponds to the slowest diffusion, is observed in $MgSO_4$, which is the least conductive from the investigated electrolytes (31.2 mS cm^{-1}, see Table S1, SM). The highest area under the CV curve, which corresponds to the highest capacitance value was recorded in sulphuric acid (80.5 mF cm^{-2} at 100 mV s^{-1}) and the lowest in magnesium sulphate (37.2 mF cm^{-2}). The capacitance values obtained in lithium, sodium and potassium sulphates equal to 45.7, 45.4 and 50.6 mF cm^{-2}, respectively. Taking into account the thickness of our composite films [29], the maximum capacitance achieved is equal to 933 F cm^{-3} (at 5 mV s^{-1} in 0.5 M H_2SO_4), which is considerably higher than reported for similar ternary composite (761 F cm^{-3} at 5 mV s^{-1} in 1 M H_2SO_4) [50]. Comparison of electrochemical performance of various ternary composites based on conducting polymers and carbonaceous materials are presented in Table S4 (SM). The specific capacitance values calculated from CV curves are consistent with the values calculated from galvanostatic discharge curves as presented in Fig. 2b)-d).

Capacitance values increase with increasing ionic conductivity of the electrolyte (Table S1, SM) and with decreasing cation size (Tables S2 and S3, SM). The highest capacity obtained in acidic solution may also be caused by additional redox reactions of surface functional groups present of oxidised carbonaceous components of the composite. For instance, quinone/hydroquinone redox reaction is often reported to add a significant pseudocapacitive contribution to the total capacitance of carbon electrodes in protic electrolytes [11,51–53]. Another reason for the higher capacitance in acidic media, may be explained by a better electrical conductivity of PEDOT in acidic solution due to improved transformation of the benzoid to quinoid structure of the PEDOT chains [54].

These results are in agreement with the data obtained by Zhu et al. for polypyrrole/reduced graphene oxide (PPY/GOx) composite in various aqueous chloride electrolytes [18]. The authors explain that the capacitance values for PPY/GOx increased with the increasing cationic mobility ($Li^+ < Na^+ < K^+ < H^+$) due to its impact on the ionic conductivity.

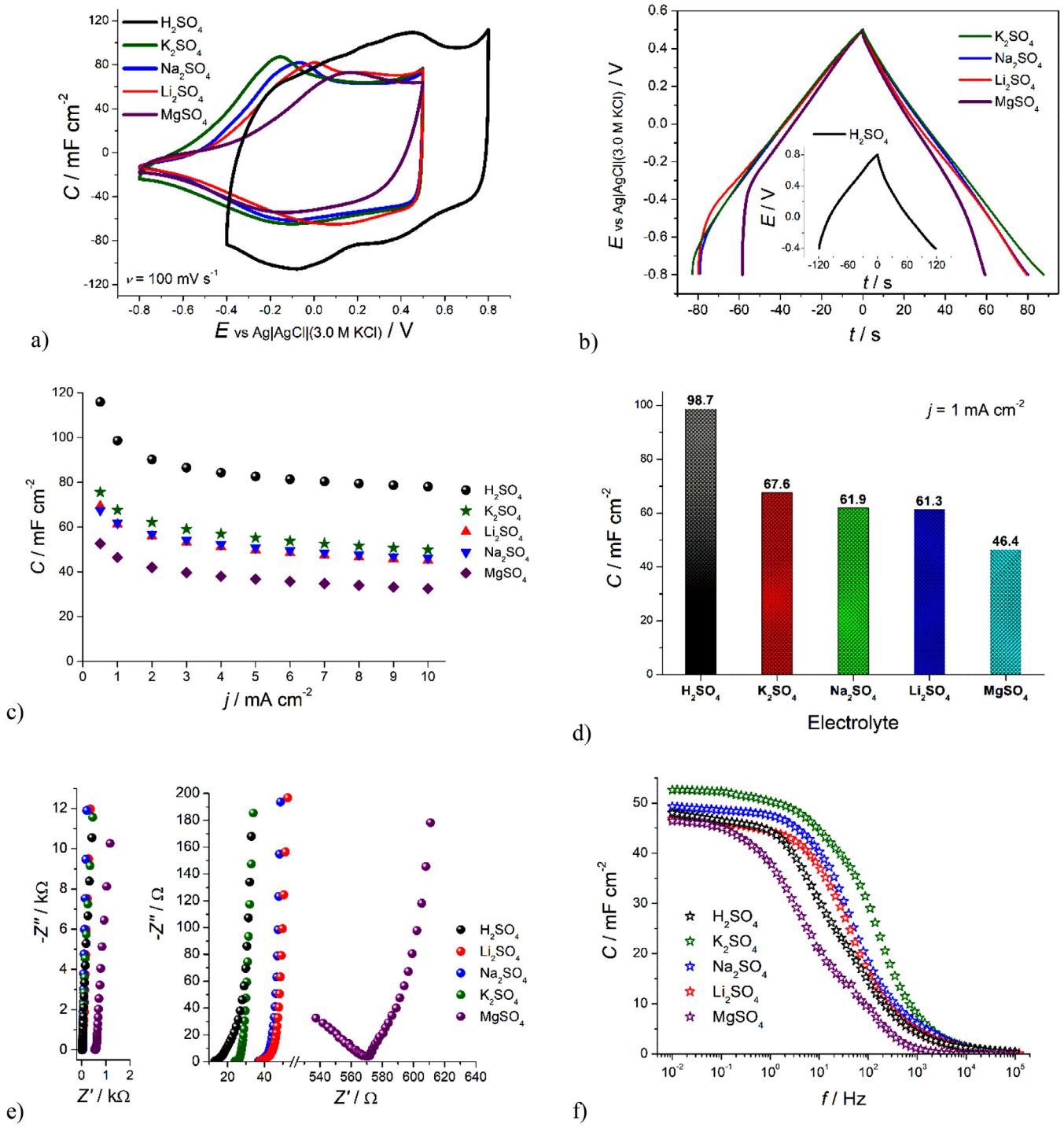

Fig. 2. Electrochemical performance of PEDOT/GOx/oxMWCNTs in various 0.5 M sulphate aqueous electrolytes in a three-electrode setup: cyclic voltammetry recorded at 100 mV s^{-1} (a); chronopotentiometry curves recorded at 1 mA cm^{-2} (b); capacitance values calculated from chronopotentiometry curves recorded at various current densities (c) and at 1 mA cm^{-2} (d); Nyquist plots (e); the relation between capacitance and frequency (f).

In all investigated electrolytes PEDOT/GOx/oxMWCNTs composite shows an excellent rate capability (Fig. 2c). Capacitance values are the highest in H_2SO_4, but the rate capability is inferior in acidic solution compared to the neutral ones. The lowest capacitance values were obtained in $MgSO_4$ (1.46 times smaller than in K_2SO_4 and more than two times smaller than in H_2SO_4 at 1 mA cm^{-2} current rate). Electrochemical impedance data also illustrate influence of ionic conductivity of the electrolytes. The highest contact resistance at the interface of electrolyte and composite layer was recorded in $MgSO_4$, as presented in Nyquist plots (Fig. 2e). Capacitance as a function of frequency (Fig. 2f) shows the best charge propagation for electrode material operating in 0.5 M K_2SO_4. The almost horizontal dependence of the capacitance vs frequency was observed in the range of 0.010 - 10 Hz in K_2SO_4 electrolyte and only 0.010- 0.2 Hz in $MgSO_4$.

Electrochemical tests of the composites were also measured in symmetric devices. For this purpose two PEDOT/GOx/oxMWCNTs layers electrodeposited on glassy carbon substrate were separated

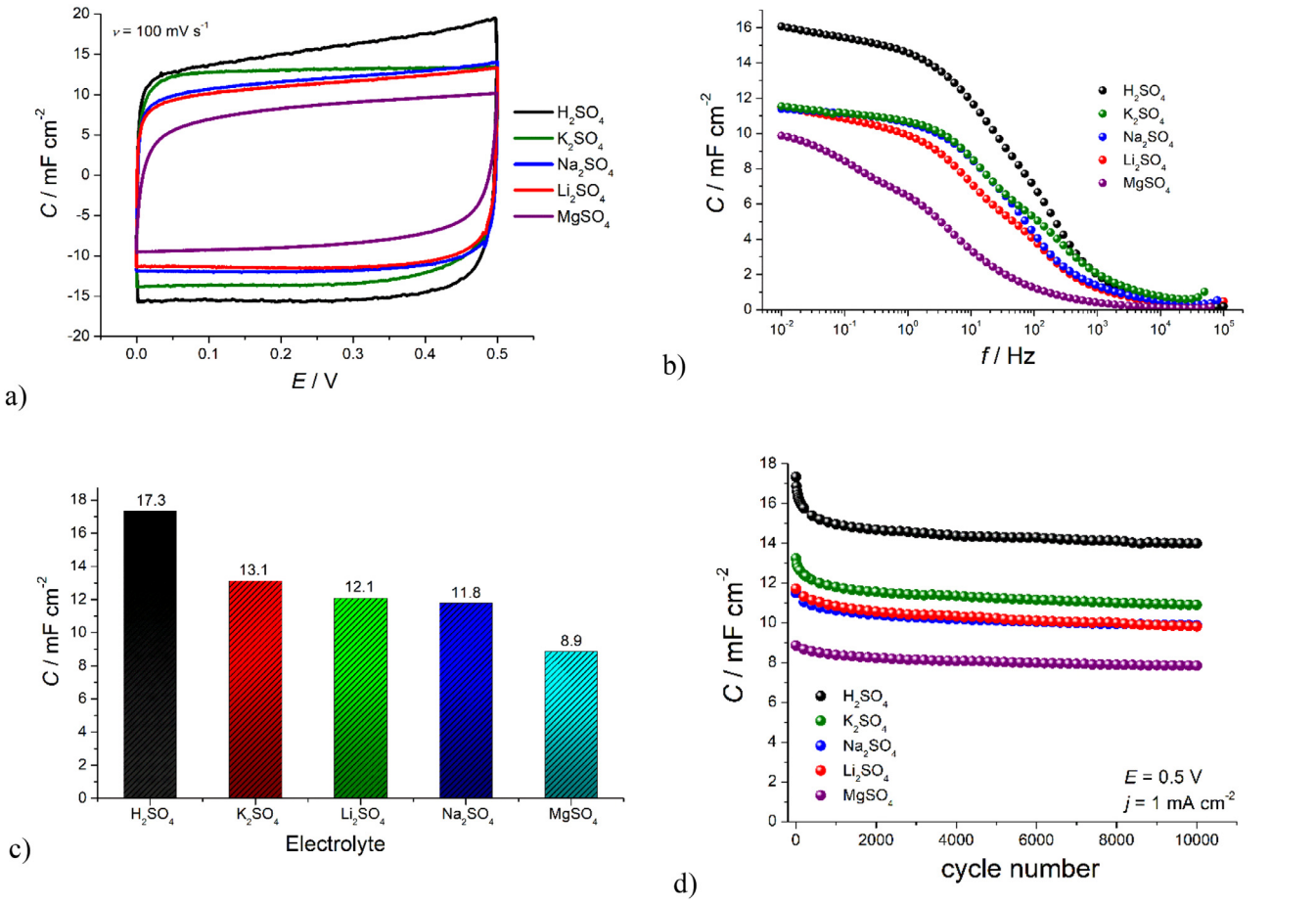

Fig. 3. Cyclic voltammetry curves recalculated into capacitance values (a); capacitance dependence on frequency (b); capacitance values calculated from chronopotentiometry at 1 mA cm^{-2} and 0.5 V (c); cycling stability during prolonged charge/discharge at 1 mA cm^{-2} and 0.5 V (d).

with glass-fibre filter paper soaked with the electrolyte and assembled in the Swagelok®-type cell. The capacitance values for the symmetric supercapacitors were calculated based on the following techniques: cyclic voltammetry (Fig. 3a), electrochemical impedance spectroscopy (Fig. 3b), chronopotentiometry at 1 mA cm^{-2} (Fig. 3c) and prolonged charging/discharging for 10′000 cycles (Fig. 3d).

CV curves at 100 mV s^{-1} in the tested cell voltage 0.5 V, are rectangular in shape indicating good capacitive properties of the electrode material. The deviation of CV curve recorded in $MgSO_4$ is smaller in comparison to the three-electrode system. The capacitance recorded in the sulphuric acid electrolyte is the highest and equal to 17.3 mF cm^{-2}. In comparison, the capacitance recorded in $MgSO_4$ (8.9 mF cm^{-2}) is almost two times smaller than in H_2SO_4 and 32% smaller than in K_2SO_4 (13.1 mF cm^{-2}). The highest cycling stability during 10′000 cycles was achieved in $MgSO_4$ (88.4% of initial capacitance value after 10′000 cycles) and the lowest for H_2SO_4 - 80.7%. The cycling stabilities of the capacitors in sulphate electrolytes with K^+, Na^+ and Li^+ cations are equal to 82.4%, 85.9% and 83.8%, respectively. For comparison, cycling stability reported for PPY/GOx by Zhu et al. [18] was the highest in acidic solution (3 M HCl), and was decreasing with increasing cation size (H^+ < Li^+ < Na^+ < K^+), which was attributed to a decrease of doping level and structural damage by insertion and de-insertion of large cations upon cycling. In the case of our ternary composites, the presence of carbon nanotubes may support mechanical strength of the composite, resulting in the good stability upon prolonged insertion and de-insertion of large ions such as K^+.

The capacitive effects was characterized by analysing the cyclic voltammetry data at various scan rates 2–500 mV s^{-1}. The measured current is related to the scan rate via the power law according to Eq. (1) proposed by Lindström et al. [55]:

$$i = a \cdot \nu^b \quad (1)$$

where: i – is current, ν – is scan rate, a and b - are adjustable parameters, that can be obtained after fitting the linear dependence given in (Eq. (2)):

$$\ln(i) = \ln(a) + b \cdot \ln(\nu) \quad (2)$$

These equations can be used to determine the presence of capacitive and semi-infinite diffusion-controlled kinetics of the electrode processes. The b-value delivers quantitative information about kinetics limitations; when current is diffusion limited $b = 0.5$, and when the current is directly proportional to the sweep rate the process is surface-controlled (capacitive) $b = 1$. In the case that b parameter falls between 0.5 and 1, the electrode mechanism is a combination of capacitive and diffusion contributions [36] or finite-length diffusion controlled [56].

Hence, in an ideal case for supercapacitors b parameter is close to 1, whereas for batteries b equals to ~0.5. By virtue of charge storage mechanism one can distinguish between both devices. In the case of PEDOT/GOx/oxMWCNTs-based supercapacitor tested in K_2SO_4 electrolyte b is in the range of 0.951–977 (Fig. 4) in the tested voltage range 0–0.5 V, indicating that the charge storage mechanism is predominantly non-diffusion-limited, namely fast surface oxidation/reduction processes and adsorption of ions.

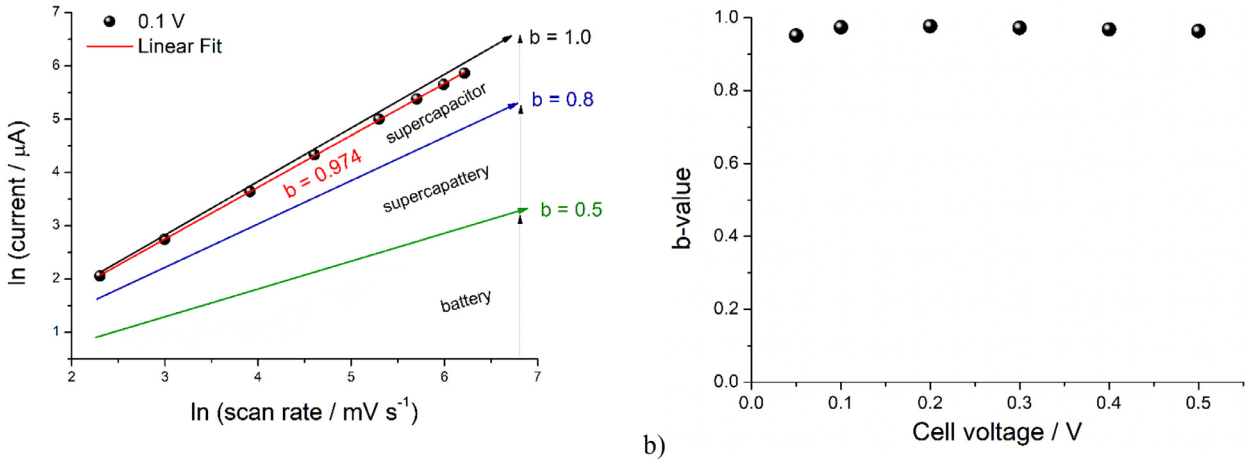

Fig. 4. Distinguishing the nature of the device by calculation of the *b* parameter from the power law – slope of the linear dependence of the ln of current vs ln of scan rate at 0.1 V cell voltage (a). Values of *b* parameters at different cell voltage (b).

A linear combination of non-diffusion and diffusion-controlled currents was proposed by Conway [36]:

$$i(V) = k_1 \cdot \nu + k_2 \cdot \nu^{1/2} \tag{3}$$

$$\frac{i(V)}{\nu^{1/2}} = k_1 \cdot \nu^{1/2} + k_2 \tag{4}$$

where: k_1 and k_2 are constants that can be calculated from current response at certain potentials across the multiple sweep rates. The analysis enables the division of the cyclic voltammograms into non-diffusion (surface)-controlled and diffusion-controlled regions. This approach was used by Dunn et al. for analysing the charge storage mechanism in many types of nanostructured transition metal oxides [57–59].

Fig. 5a-d) presents cyclic voltammograms at various scan rates with marked capacitive contribution recorded for PEDOT/GOx/oxMWCNTs symmetric capacitor with K_2SO_4 as electrolyte. At lower scan rates, non-diffusive contribution is slightly lower than at high scan rates. Linear fitting of k_1 and k_2 parameters are shown in Fig. 5e). It can be noticed that at close to boundary cell voltages (0 and 0.5 V) points at high scan rates slightly deviate from linear trend. This is attributed to Ohmic losses due to internal resistance of the cell. Diffusive and non-diffusive contribution at sweep rates from 10 to 500 mV s^{-1} are depicted in Fig. 5f).

Another approach to differentiate capacitive and diffusive contributions to the total capacitance value is Trasatti's analysis [34][35]. According to this method, the total amount of the charge stored (q_T) is a sum of inner (less accessible) surface charge (q_i) and outer (more accessible) surface charge (q_o) according to Eq. 5:

$$q_T = q_i + q_o \tag{5}$$

The charge stored at the inner surface is controlled by diffusion, whereas outer surface charge is non-diffusion controlled, therefore it is independent of scan rate. The charge measured at certain scan rate (q_v) can be expressed by the following equations [34][35]:

$$q_v = q_\infty + const. \cdot \nu^{1/2} \tag{6}$$

$$\frac{1}{q_v} = \frac{1}{q_0} + const.' \cdot \nu^{1/2} \tag{7}$$

where: q_∞ is the charge stored at extremely high scan rates ($\nu \to \infty$) and q_0 is the charge stored at a very slow scan rate ($\nu \to 0$); q_∞ is assumed to be equal to the outer surface charge q_o, while q_0 is assumed to be equal to the total charge q_T stored at the electrode.

Taking into account the cell voltage one can express the above equations as capacitance values (C_T and C_o are calculated from q_T and q_o, respectively) as presented in Fig. 6 for PEDOT/GOx/oxMWCNTs symmetric capacitor with K_2SO_4 electrolyte. Presented data were linearly fitted in the sweep rate range of 10–500 mV s^{-1}. For low scan rates the inner surface charge contribution in the total charge is higher than for the high scan rates (11.3% at 10 mV s^{-1}, and 0.6% at 400 mV s^{-1}). The inner- and outer-surface capacitance contribution corresponding to diffusion controlled and non-diffusion controlled processes are in agreement with the values calculated using Eq. (4) (presented in Fig. 5f).

Note that both methods give convergent results (see Fig. 5f and Fig. 6c). The data were fitted linearly in the broad scan rate range of 10–500 mV s^{-1}. In literature reports, high scan rates are often excluded from linear fitting due to Ohmic drops resulting from intrinsic resistance [60–62]. One has to bear in mind that fitting in various ranges of scan rate will give slightly different results, as presented in Fig. 7 for PEDOT/GOx/oxMWCNTs symmetric capacitor with 0.5 M $MgSO_4$ as electrolyte. The corresponding linear fitting of k_1 and k_2 parameters are shown in Fig. S2 (SM). Analysis utilizing Trasatti's method taking into account various scan rate ranges is presented in Fig. S3 (SM). C_o/C_T values corresponding to non-diffusion controlled contribution are equal to 84.8, 73.7 and 64.3% for linear fitting in the range of 2–20, 2–100 and 10–100 mV s^{-1}, respectively.

To show the influence of cation type on the electrochemical behaviour of PEDOT/GOx/oxMWCNTs composite, the analyses were performed for symmetric capacitors with H_2SO_4, Li_2SO_4, Na_2SO_4, K_2SO_4 and $MgSO_4$ electrolytes (Fig. 8). For these analyses we excluded the highest sweep rates from the linear fitting and did the calculations for the range of 10–100 mV s^{-1}. Symmetric capacitor with magnesium sulphate as electrolyte exhibits the highest diffusion controlled contribution to capacitance values. According to Table S2 (SM) Mg^{2+} ions have the lowest bare and hydrated ion size, similar to Li^+ ions, so the highest diffusive contribution recorded in $MgSO_4$ may be attributed to the lowest ionic conductivity of this electrolyte (Table S1 (SM)), which is connected with a formation by Mg^{2+} and SO_4^{2-} ions extensive water-separated, hence strongly dipolar, ion pairs [42]. H_2SO_4 has the highest conductivity (from 2.6 to 6.3 times higher than investigated neutral electrolytes), which results from different mechanism of proton transport. However, the diffusion-controlled contribution is much higher in H_2SO_4 than in K_2SO_4 (15.3% vs 7.5%). Such difference may

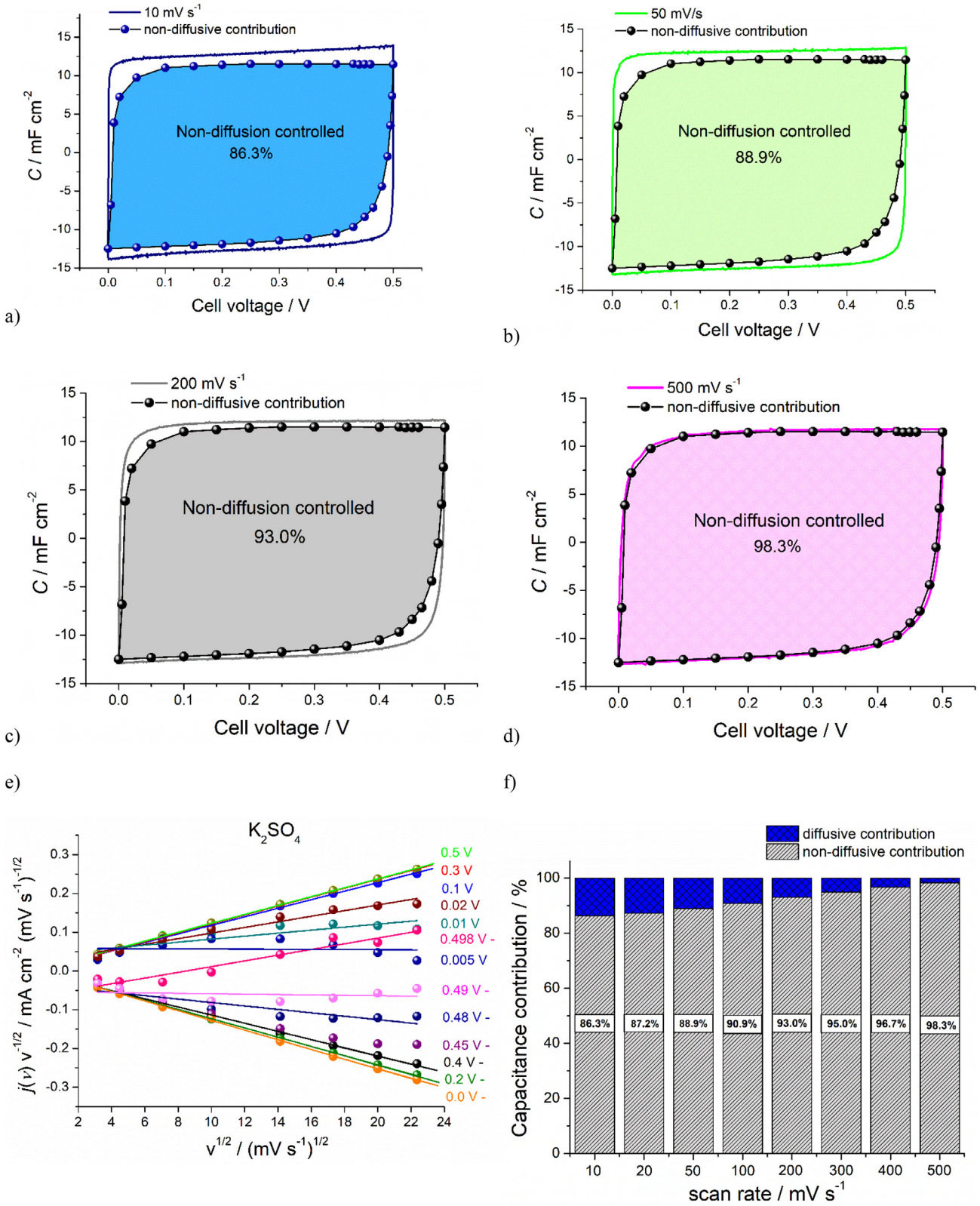

Fig. 5. CV curves with marked non-diffusion controlled contribution in the total capacitance calculated using Eq. 4: 10 mV s^{-1} (a), 50 mV s^{-1} (b), 200 mV s^{-1} (c), 500 mV s^{-1}(d). Linear fitting of the k_1 and k_2 parameters in the sweep rate range of 10–500 mV s^{-1} (e). Diffusion controlled and non-difussion controlled contribution to total capacitance at various scan rates (f).

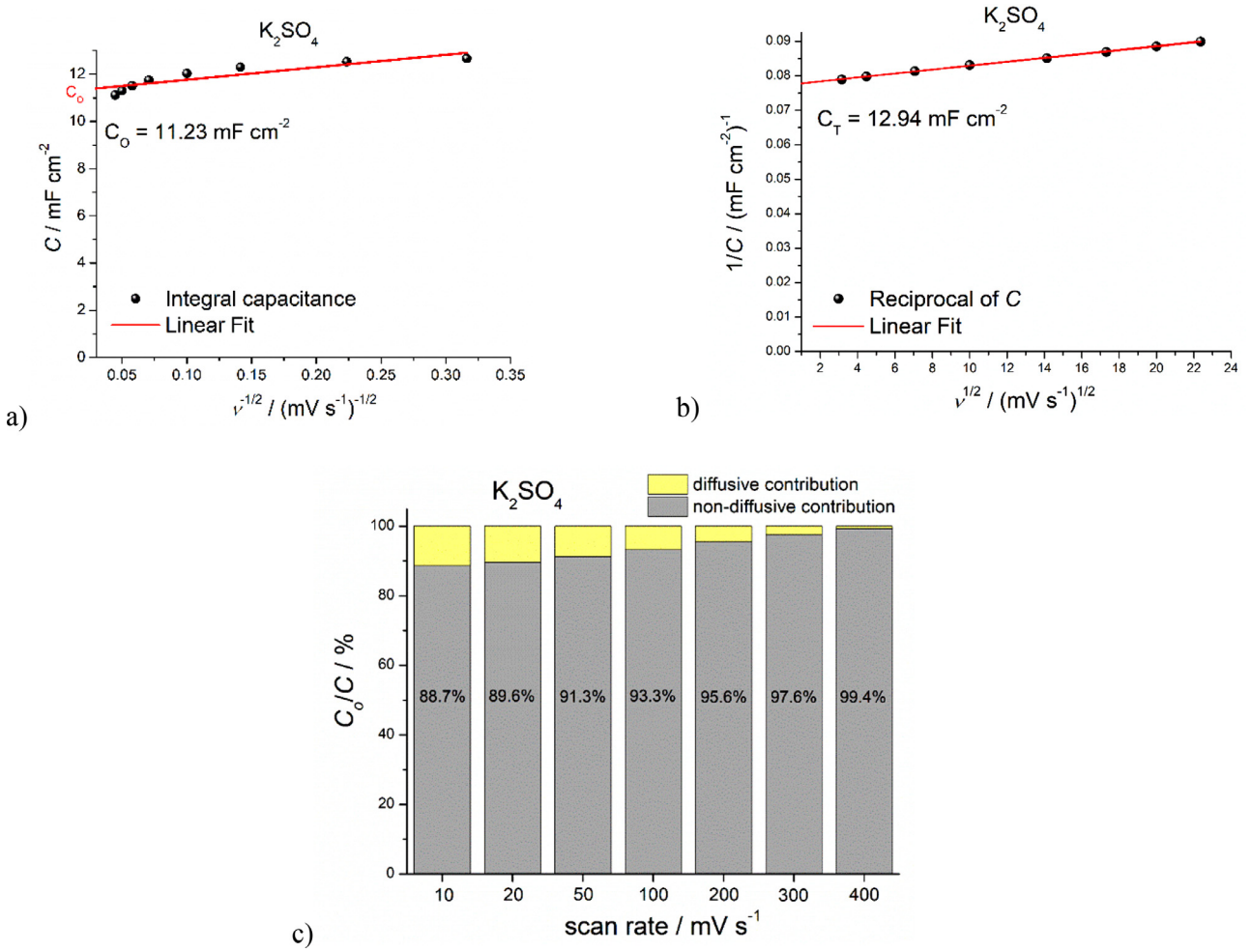

Fig. 6. Extrapolation of C_o value (a); extrapolation of C_T value (b); contribution of outer- and inner-surface capacitance at variuos sweep rates (c).

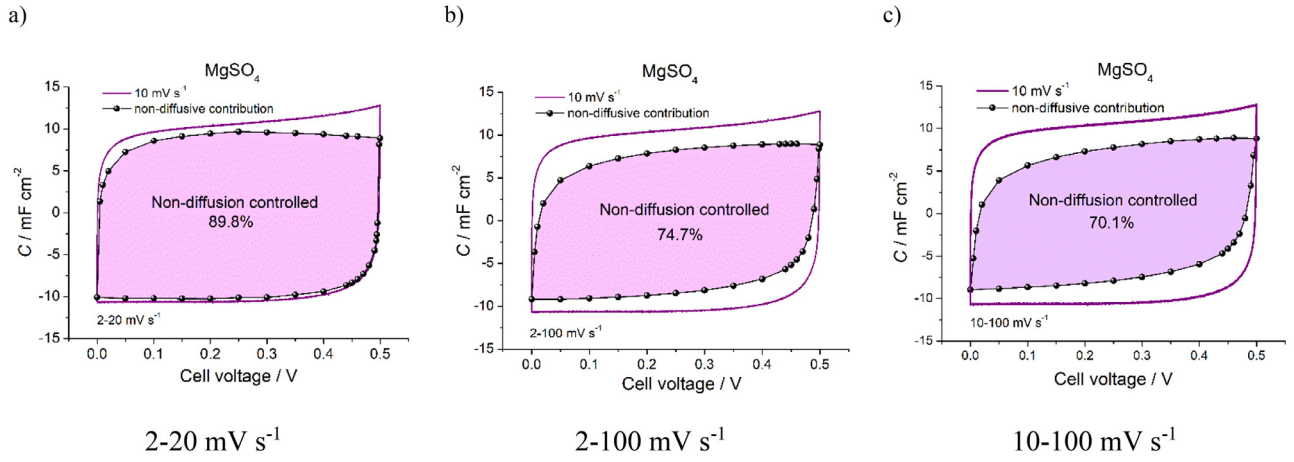

Fig. 7. Non-diffusive contribution to capacitance value calculated using Conway and Dunn's method taking into account selected scan rate range: a) 2–20 mV s^{-1}, b) 2–100 mV s^{-1}, c) 10–100 mV s^{-1}.

be explained by the occurrence of diffusion-controlled redox reactions of oxygen-rich functional groups (e.g. quinone or hydroxyl), present on the surface of graphene oxide and oxidised CNTs, which are more pronounced in acidic media [11,51–53]. This would explain not only higher diffusion-controlled contribution but also significantly higher capacitance for PEDOT/GOx/oxMWCNTs recorded in acidic solution compared to the neutral one.

Analyses according to both presented methods show that PEDOT/GOx/oxMWCNTs composites operating in symmetric device exhibit mainly capacitive character of the charge storage mechanism, especially in K_2SO_4 electrolyte. For comparison, Nadevi et al. [7] reported analyses to determine charge transfer mechanism for rGOx-PEDOT:PSS/MnO_2 and rGOx-PEDOT:PSS electrodes in 1 M Na_2SO_4 electrolyte. The *b*-value was equal to 0.6 and 0.8 for

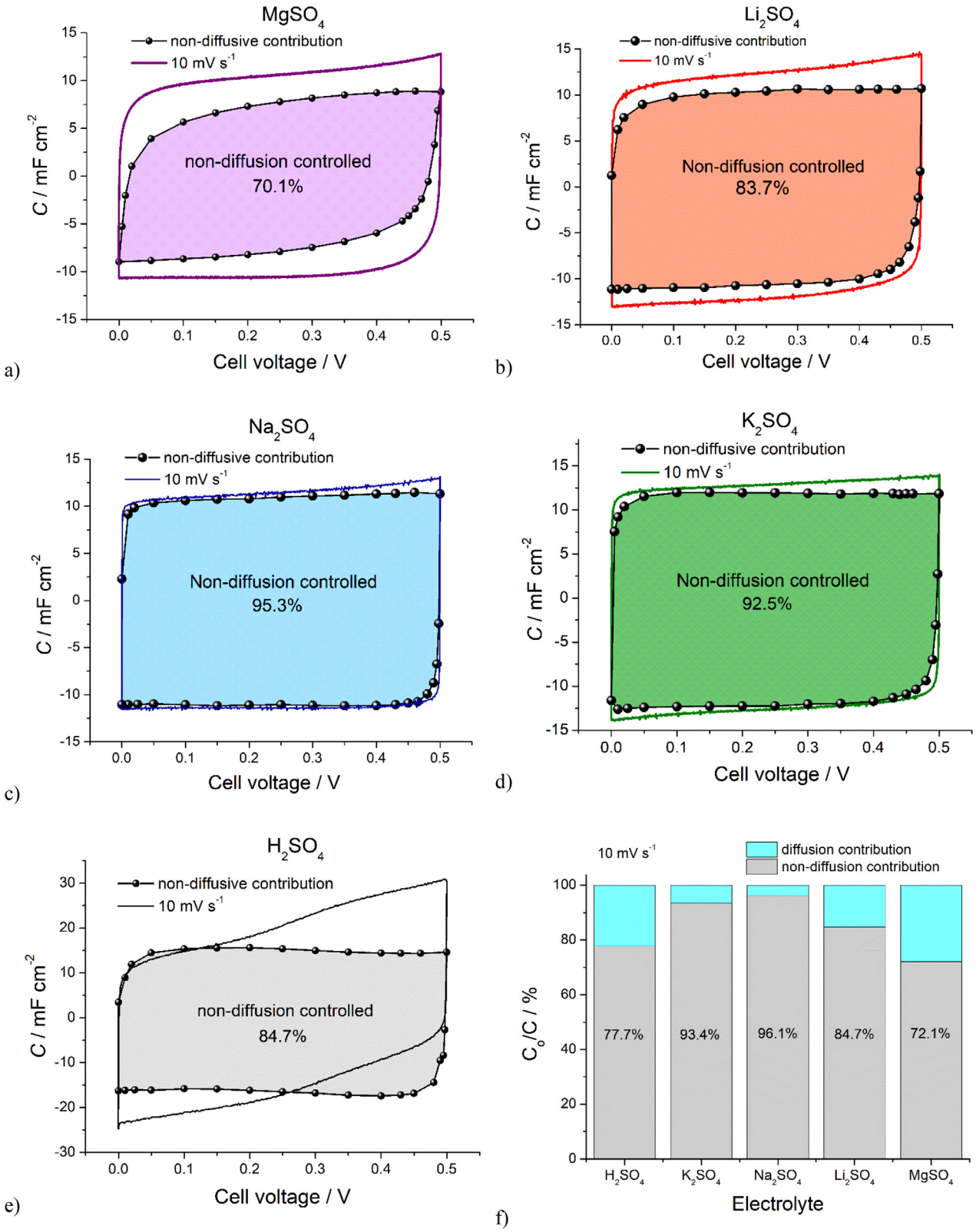

Fig. 8. The comparison of non-diffusion contribution to capacitance of PEDOT/GOx/oxMWCNTs symmetric capacitors for CV at 10 mV s^{-1} scan rate recorded in different electrolytes: (a)-(e) calculated from Conway's equation Eq. (4)), (f) calculated from Trasatti's equations (Eq. (5)-(7). Linear fitting were performed for the scan range of 10–100 mV s^{-1}.

rGOx-PEDOT:PSS/MnO_2 and rGOx-PEDOT:PSS, respectively, meaning mainly diffusion controlled kinetics for electrode with manganese oxide component (66% of diffusive contribution to capacitance at 20 mV s^{-1} according to analysis with Conway's equation). Trasatti method resulted in diffusion controlled contribution (inner surface charge) of 66% and 71% for rGOx-PEDOT:PSS/MnO_2 and rGOx-PEDOT:PSS electrodes, respectively. Boota and Gogotsi [63] investigated asymmetric capacitors based on M-Xene as negative electrodes and various conducting polymer/graphene oxide composites as positive electrode. Capacitors with PANI/GOx, PPY/GOx or PEDOT/GOx as positive electrode exhibited, 93, 86 and 68% of non-diffusion-controlled contribution, respectively, calculated utilizing Conway's equation. This shows that the type of electroactive polymer influence significantly the charge storage mechanism of the device. On the other hand, doping ion type in the polymer matrix is also crucial for charge storage kinetics. For instance, Szkoda et al. [64] by changing counter ion in PANI films from chlorides to exfoliated WO_{3-x}, increased capacitive contribution from 28 to 54% at 5 mV s^{-1}, and from 59 to 78% at 100 mV s^{-1} recorded in 1 M H_2SO_4 electrolyte.

Conclusions

Ternary composite PEDOT/GOx/oxMWCNTs was tested as electrode material in symmetric capacitors in various aqueous electrolytes. The Trasatti's analysis as well as Conway 's equation were implemented to differentiate between diffusion-related and non-diffusion-related capacitance. The importance of proper selection of sweep rate range for the linear fitting and extrapolation of parameters was pointed out. The results show that the investigated composite exhibits mainly capacitive behaviour and fast kinetics of electrode processes in all tested electrolytes. The highest capacitance value was recorded in acidic solution, which can be attributed to the additional redox reactions of oxygen-rich functional groups on the surface of GOx and ox-CNTs. The utmost influence on the capacitance values was related to the viscosity and conductivity of the electrolyte, hence significantly lower values recorded in $MgSO_4$ electrolyte. Despite the lower size of the magnesium cation compared to lithium, sodium and potassium ions, the capacitance obtained in $MgSO_4$ is lower than in other investigated electrolytes with cations of larger sizes.

Declaration of Competing Interest

The authors declare that they have no known competing financial interests or personal relationships that could have appeared to influence the work reported in this paper.

Credit authorship contribution statement

Anita Cymann-Sachajdak: Investigation, Methodology, Formal analysis, Visualization, Writing - original draft, Writing - review & editing. **Magdalena Graczyk-Zajac:** Formal analysis, Writing - original draft, Writing - review & editing. **Grzegorz Trykowski:** Methodology, Visualization, Writing - original draft. **Monika Wilamowska-Zawłocka:** Conceptualization, Investigation, Methodology, Supervision, Formal analysis, Writing - original draft, Writing - review & editing, Funding acquisition.

Acknowledgements

The authors thank Prof. Joanna Krakowiak (Gdańsk University of Technology) for fruitful discussions concerning properties of electrolytes.

Funding sources

This work was supported by Foundation for Polish Science under REINTEGRATION programme [Grant No. POIR.04.04.00-00-4582/17-00].

Supplementary materials

Supplementary material associated with this article can be found, in the online version, at doi:10.1016/j.electacta.2021.138356.

Appendices

Supplementary Materials provides additional information on: *i)* properties of electrolytes, *ii)* calculations of diffusion controlled and non-diffusion controlled contribution to capacitance taking into account various scan rate ranges and *iii)* comparison of electrochemical performance of ternary composites based on various conducting polymers.

References

[1] C. Decaux, C. Matei Ghimbeu, M. Dahbi, M. Anouti, D. Lemordant, F. Béguin, C. Vix-Guterl, E. Raymundo-Piñero, Influence of electrolyte ion-solvent interactions on the performances of supercapacitors porous carbon electrodes, J. Power Sources 263 (2014) 130–140, doi:10.1016/j.jpowsour.2014.04.024.
[2] M. Marcinek, J. Syzdek, M. Marczewski, M. Piszcz, L. Niedzicki, M. Kalita, A. Plewa-Marczewska, A. Bitner, P. Wieczorek, T. Trzeciak, M. Kasprzyk, P. Łężak, Z. Zukowska, A. Zalewska, W. Wieczorek, Electrolytes for Li-ion transport – review, Solid State Ionics 276 (2015) 107–126, doi:10.1016/j.ssi.2015.02.006.
[3] A. Ponrouch, R. Dedryvère, D. Monti, A.E. Demet, J.M. Ateba Mba, L. Croguennec, C. Masquelier, P. Johansson, M.R. Palacín, Towards high energy density sodium ion batteries through electrolyte optimization, Energy Environ. Sci. 6 (2013) 2361–2369, doi:10.1039/c3ee41379a.
[4] H. Tomiyasu, H. Shikata, K. Takao, N. Asanuma, S. Taruta, Y.Y. Park, An aqueous electrolyte of the widest potential window and its superior capability for capacitors, Sci. Rep. 7 (2017) 1–12, doi:10.1038/srep45048.
[5] J.H. Chae, G.Z. Chen, 1.9V aqueous carbon-carbon supercapacitors with unequal electrode capacitances, Electrochim. Acta 86 (2012) 248–254, doi:10.1016/j.electacta.2012.07.033.
[6] K. Fic, G. Lota, M. Meller, E. Frackowiak, Novel insight into neutral medium as electrolyte for high-voltage supercapacitors, Energy Environ. Sci. 5 (2012) 5842–5850, doi:10.1039/c1ee02262h.
[7] L. Naderi, S. Shahrokhian, F. Soavi, Fabrication of a 2.8 v high-performance aqueous flexible fiber-shaped asymmetric micro-supercapacitor based on MnO2/PEDOT:pSS-reduced graphene oxide nanocomposite grown on carbon fiber electrode, J. Mater. Chem. A 8 (2020) 19588–19602, doi:10.1039/d0ta06561g.
[8] J. Chmiola, C. Largeot, P.L. Taberna, P. Simon, Y. Gogotsi, Desolvation of ions in subnanometer pores and its effect on capacitance and double-layer theory, Angew. Chemie - Int. Ed. 47 (2008) 3392–3395, doi:10.1002/anie.200704894.
[9] R. Mancinelli, A. Botti, F. Bruni, M.A. Ricci, A.K. Soper, Hydration of sodium, potassium, and chloride ions in solution and the concept of structure maker/breaker, J. Phys. Chem. B 111 (2007) 13570–13577, doi:10.1021/jp075913v.
[10] K. Nanaji, T.N. Rao, U.V. Varadaraju, S. Anandan, Pore size-engineered three-dimensional ordered mesoporous carbons with improved electrochemical performance for supercapacitor and lithium-ion battery applications, ChemistrySelect 4 (2019) 10104–10112, doi:10.1002/slct.201902237.
[11] M. Seredych, M. Koscinski, M. Sliwinska-Bartkowiak, T.J. Bandosz, Active pore space utilization in nanoporous carbon-based supercapacitors: effects of conductivity and pore accessibility, J. Power Sources 220 (2012) 243–252, doi:10.1016/j.jpowsour.2012.07.074.
[12] G. Inzelt, M. Pineri, J.W. Schultze, M.A. Vorotyntsev, Electron and proton conducting polymers: recent developments and prospects, Electrochim. Acta 45 (2000) 2403–2421, doi:10.1016/S0013-4686(00)00329-7.
[13] A. Pron, P. Rannou, Processible conjugated polymers: from organic semiconductors to organic metals and superconductors, Prog. Polym. Sci. 27 (2002) 135–190, doi:10.1016/S0079-6700(01)00043-0.
[14] M. Skompska, J. Mieczkowski, R. Holze, J. Heinze, In situ conductance studies of p- and n-doping of poly(3,4- dialkoxythiophenes), J. Electroanal. Chem. 577 (2005) 9–17, doi:10.1016/j.jelechem.2004.11.008.
[15] A. Bund, S. Neudeck, Effect of the solvent and the anion on the doping/dedoping behaviour of Poly (3, 4-ethylenedioxythiophene), films studied with the electrochemical quartz microbalance, (2004) 17845–17850. doi:10.1021/jp0469721.
[16] K. Maksymiuk, K. Doblhofer, Kinetics and mechanism of charge-transfer reactions between conducting polymers and redox ions in electrolytes, Electrochim. Acta. 39 (1994) 217–227.

[17] A. Lisowska-Oleksiak, A. Kupniewska, Transport of alkali metal cations in poly (3, 4-ethylenethiophene) films, Solid State Ionics 157 (2003) 241–248.
[18] J. Zhu, Y. Xu, J. Wang, J. Lin, X. Sun, S. Mao, The effect of various electrolyte cations on electrochemical performance of polypyrrole/RGO based supercapacitors, Phys. Chem. Chem. Phys. 17 (2015) 28666–28673, doi:10.1039/c5cp04080a.
[19] V.T. Gruia, A. Ispas, I. Efimov, A. Bund, Cation exchange behaviour during the redox switching of poly (3,4-ethylenedioxythiophene) films, J. Solid State Electrochem. 24 (2020) 3231–3244, doi:10.1007/s10008-020-04809-6.
[20] I. Jureviciute, S. Bruckenstein, A.R. Hillman, Cation participation during the redox switching of poly (vinylferrocene) films in aqueous 0 . 05M perchlorate solutions Part 1 : cyclic voltammetry and the EQCM, 51 (2006) 2351–2357. doi:10.1016/j.electacta.2005.02.155.
[21] A.R. Hillman, M.A. Mohamoud, I. Efimov, Time-temperature superposition and the controlling role of solvation in the viscoelastic properties of polyaniline thin films, Anal. Chem. 83 (2011) 5696–5707, doi:10.1021/ac200901d.
[22] A.R. Hillman, S.J. Daisley, S. Bruckenstein, Kinetics and mechanism of the electrochemical p-doping of PEDOT, Electrochem. Commun. 9 (2007) 1316–1322, doi:10.1016/j.elecom.2007.01.009.
[23] M.A. Vorotyntsev, E. Vieil, J. Heinze, Ionic exchange of the polypyrrole film with the PC lithium perchlorate solution during the charging process, Electrochim. Acta 41 (1996) 1913–1920, doi:10.1016/0013-4686(95)00512-9.
[24] H. Zhou, X. Zhi, Ternary composite electrodes based on poly(3,4–ethylenedioxythiophene)/carbon nanotubes–carboxyl graphene for improved electrochemical capacitive performances, Synth. Met. 234 (2017) 139–144, doi:10.1016/j.synthmet.2017.10.011.
[25] H. Zhou, H.J. Zhai, G. Han, Superior performance of highly flexible solid-state supercapacitor based on the ternary composites of graphene oxide supported poly(3,4-ethylenedioxythiophene)-carbon nanotubes, J. Power Sources 323 (2016) 125–133, doi:10.1016/j.jpowsour.2016.05.049.
[26] H. Zhou, H.J. Zhai, X. Zhi, Enhanced electrochemical performances of polypyrrole/carboxyl graphene/carbon nanotubes ternary composite for supercapacitors, Electrochim. Acta 290 (2018) 1–11, doi:10.1016/j.electacta.2018.09.039.
[27] A. Dettlaff, M. Wilamowska, Electrochemical synthesis and characterization of nanocomposites based on poly(3,4-ethylenedioxythiophene) and functionalized carbon nanotubes, Synth. Met. 212 (2016) 31–43, doi:10.1016/j.synthmet.2015.11.030.
[28] M. Wilamowska, M. Kujawa, M. Michalska, L. Lipińska, A. Lisowska-Oleksiak, Electroactive polymer/graphene oxide nanostructured composites; evidence for direct chemical interactions between PEDOT and GOx, Synth. Met. 220 (2016) 334–346, doi:10.1016/j.synthmet.2016.07.002.
[29] A. Cymann, M. Sawczak, J. Ryl, E. Klugmann-Radziemska, M. Wilamowska-Zawlocka, Capacitance enhancement by incorporation of functionalised carbon nanotubes into Poly(3,4-Ethylenedioxythiophene)/Graphene oxide composites, Materials (Basel) 13 (2020) 2419, doi:10.3390/ma13102419.
[30] C. Lei, P. Wilson, C. Lekakou, Effect of poly(3,4-ethylenedioxythiophene) (PEDOT) in carbon-based composite electrodes for electrochemical supercapacitors, J. Power Sources 196 (2011) 7823–7827, doi:10.1016/j.jpowsour.2011.03.070.
[31] X. Mao, W. Yang, X. He, Y. Chen, Y. Zhao, Y. Zhou, Y. Yang, J. Xu, The preparation and characteristic of poly (3,4-ethylenedioxythiophene)/reduced graphene oxide nanocomposite and its application for supercapacitor electrode, Mater. Sci. Eng. B Solid-State Mater. Adv. Technol. 216 (2017) 16–22, doi:10.1016/j.mseb.2016.10.002.
[32] Z. Mousavi, J. Bobacka, A. Lewenstam, A. Ivaska, Poly(3,4-ethylenedioxythiophene) (PEDOT) doped with carbon nanotubes as ion-to-electron transducer in polymer membrane-based potassium ion-selective electrodes, J. Electroanal. Chem. 633 (2009) 246–252, doi:10.1016/j.jelechem.2009.06.005.
[33] P. Xiong, J. Zhu, X. Wang, Recent advances on multi-component hybrid nanostructures for electrochemical capacitors, J. Power Sources 294 (2015) 31–50, doi:10.1016/j.jpowsour.2015.06.062.
[34] S. Ardizzone, G. Fregonara, S. Trasatti, “ Inner ” and “ outer ” active surface electrodes of RuO2 electrodes, Electrochim. Acta. 35 (1990) 263–267.
[35] D. Baronetto, N. Krstajic, S. Trasatti, Reply to “note on a method to interrelate inner and outer electrode areas” by H. Vogt*, Electrochim. Acta. 39 (1994) 2359–2362, doi:10.1016/0013-4686(94)85077-1.
[36] T.-C. Liu, W.G. Pell, B.E. Conway, S.L. Roberson, Behaviour of molybdenum nitrides as materials for electrochemical capacitors: comparison with ruthenium oxide, J. Electrochem. Soc. 145 (1998) 1882–1888, doi:10.1149/1.1838571.
[37] A.G. Guex, J.L. Puetzer, A. Armgarth, E. Littmann, E. Stavrinidou, E.P. Giannelis, G.G. Malliaras, M.M. Stevens, Highly porous scaffolds of PEDOT:PSS for bone tissue engineering, Acta Biomater. 62 (2017) 91–101, doi:10.1016/j.actbio.2017.08.045.
[38] A. Dettlaff, P.R. Das, L. Komsiyska, O. Osters, J. Łuczak, M. Wilamowska-Zawłocka, Electrode materials for electrochemical capacitors based on poly(3,4 ethylenedioxythiophene) and functionalized multi-walled carbon nanotubes characterized in aqueous and aprotic electrolytes, Synth. Met. 244 (2018) 80–91, doi:10.1016/j.synthmet.2018.07.006.
[39] M. Ates, Y. Bayrak, H. Ozkan, O. Yoruk, M. Yildirim, O. Kuzgun, Synthesis of rGO/TiO 2 /PEDOT nanocomposites, supercapacitor device performances and equivalent electrical circuit models, J. Polym. Res. 26 (2019), doi:10.1007/s10965-018-1692-2.
[40] E. Gileadi, E. Kirowa-Eisner, Electrolytic conductivity-the hopping mechanism of the proton and beyond, Electrochim. Acta 51 (2006) 6003–6011, doi:10.1016/j.electacta.2006.03.084.
[41] T. Miyake, M. Rolandi, Grotthuss mechanisms: from proton transport in proton wires to bio-protonic devices, J. Phys. Condens. Matter 28 (2016) 23001, doi:10.1088/0953-8984/28/2/023001.
[42] S.I. Mamatkulov, K.F. Rinne, R. Buchner, R.R. Netz, D.J. Bonthuis, Water-separated ion pairs cause the slow dielectric mode of magnesium sulfate solutions, J. Chem. Phys. 148 (2018), doi:10.1063/1.5000385.
[43] M. Madekufamba, P.R. Tremaine, Ion association in dilute aqueous magnesium sulfate and nickel sulfate solutions under hydrothermal conditions by flow conductivity measurements, J. Chem. Eng. Data 56 (2011) 889–898, doi:10.1021/je100729t.
[44] Y. Marcus, Ionic radii in aqueous solutions, Chem. Rev. 88 (1988) 1475–1498, doi:10.1021/cr00090a003.
[45] Y. Marcus, A simple empirical model describing the thermodynamics of hydration of ions of widely varying charges, sizes, and shapes, Biophys. Chem. 51 (1994) 111–127, doi:10.1016/0301-4622(94)00051-4.
[46] Y. Marcus, H. Donald Brooke Jenkins, L. Glasser, Ion volumes: a comparison, J. Chem. Soc. Dalt. Trans. 20 (2002) 3795–3798, doi:10.1039/b205785a.
[47] B.E. Conway, E. Ayranci, Effective ionic radii and hydration volumes for evaluation of solution properties and ionic adsorption, J. Solution Chem. 28 (1999) 163–192, doi:10.1023/A:1021702230117.
[48] J. Mähler, I. Persson, A study of the hydration of the alkali metal ions in aqueous solution, Inorg. Chem. 51 (2012) 425–438, doi:10.1021/ic2018693.
[49] N. Ohtomo, K. Arakawa, Neutron diffraction study of aqueous ionic solutions. I. Aqueous solutions of lithium chloride and caesium chloride, Bull. Chem. Soc. Jpn. 52 (1979) 2755–2759, doi:10.1246/bcsj.52.2755.
[50] M.M. Islam, S.H. Aboutalebi, D. Cardillo, H.K. Liu, K. Konstantinov, S.X. Dou, Self-assembled multifunctional hybrids: toward developing high-performance graphene-based architectures for energy storage devices, ACS Cent. Sci. 1 (2015) 206–216, doi:10.1021/acscentsci.5b00189.
[51] H.A. Andreas, B.E. Conway, Examination of the double-layer capacitance of an high specific-area C-cloth electrode as titrated from acidic to alkaline pHs, Electrochim. Acta 51 (2006) 6510–6520, doi:10.1016/j.electacta.2006.04.045.
[52] A. Śliwak, B. Grzyb, J. Ćwikła, G. Gryglewicz, Influence of wet oxidation of herringbone carbon nanofibers on the pseudocapacitance effect, Carbon N. Y. 64 (2013) 324–333, doi:10.1016/j.carbon.2013.07.082.
[53] K. Fic, E. Frackowiak, F. Béguin, Unusual energy enhancement in carbon-based electrochemical capacitors, J. Mater. Chem. 22 (2012) 24213–24223, doi:10.1039/c2jm35711a.
[54] Y. Xia, K. Sun, J. Ouyang, Solution-processed metallic conducting polymer films as transparent electrode of optoelectronic devices, Adv. Mater. 24 (2012) 2436–2440, doi:10.1002/adma.201104795.
[55] H. Lindström, S. Södergren, A. Solbrand, H. Rensmo, J. Hjelm, A. Hagfeldt, S.E. Lindquist, Li+ ion insertion in TiO_2 (anatase). 1. Chronoamperometry on CVD films and nanoporous films, J. Phys. Chem. B. 101 (1997) 7710–7716, doi:10.1021/jp970489r.
[56] K. Aoki, K. Tokuda, H. Matsuda, Theory of linear sweep voltammetry with finite diffusion space. Part II, Totally Irrevers. Quasi-Revers. Cases 160 (1984) 33–45.
[57] J. Wang, J. Polleux, J. Lim, B. Dunn, Pseudocapacitive contributions to electrochemical energy storage in TiO_2 (anatase) nanoparticles, J. Phys. Chem. C. 111 (2007) 14925–14931, doi:10.1021/jp074464w.
[58] K. Brezesinski, J. Wang, J. Haetge, C. Reitz, S.O. Steinmueller, S.H. Tolbert, B.M. Smarsly, B. Dunn, T. Brezesinski, Pseudocapacitive contributions to charge storage in highly ordered mesoporous group v transition metal oxides with iso-oriented layered nanocrystalline domains, J. Am. Chem. Soc. 132 (2010) 6982–6990, doi:10.1021/ja9106385.
[59] V. Augustyn, P. Simon, B. Dunn, Pseudocapacitive oxide materials for high-rate electrochemical energy storage, Energy Environ. Sci. 7 (2014) 1597–1614, doi:10.1039/c3ee44164d.
[60] S. Fleischmann, J.B. Mitchell, R. Wang, C. Zhan, D.E. Jiang, V. Presser, V. Augustyn, Pseudocapacitance: from fundamental understanding to high power energy storage materials, Chem. Rev. 120 (2020) 6738–6782, doi:10.1021/acs.chemrev.0c00170.
[61] J. Yan, C.E. Ren, K. Maleski, C.B. Hatter, B. Anasori, P. Urbankowski, A. Sarycheva, Y. Gogotsi, Flexible MXene/graphene films for ultrafast supercapacitors with outstanding volumetric capacitance, Adv. Funct. Mater. 27 (2017) 1–10, doi:10.1002/adfm.201701264.
[62] D. Shan, J. Yang, W. Liu, J. Yan, Z. Fan, Biomass-derived three-dimensional honeycomb-like hierarchical structured carbon for ultrahigh energy density asymmetric supercapacitors, J. Mater. Chem. A 4 (2016) 13589–13602, doi:10.1039/c6ta05406d.
[63] M. Boota, Y. Gogotsi, MXene—conducting polymer asymmetric pseudocapacitors, Adv. Energy Mater. 9 (2019) 1–8, doi:10.1002/aenm.201802917.
[64] M. Szkoda, Z. Zarach, K. Trzciński, A.P. Nowak, An aqueous exfoliation of wo3 as a route for counterions fabrication—improved photocatalyticand capacitive properties of polyaniline/wo3 composite, Materials (Basel) 13 (2020) 1–16, doi:10.3390/ma13245781.